SPATIALLY ADAPTIVE TOTAL VARIATION IMAGE DENOISING UNDER SALT AND PEPPER NOISE

Renán Rojas and Paul Rodriguez

Digital Signal Processing Group, Pontificia Universidad Católica del Perú
Lima, Peru
phone: + (511) 626-2000 anx 4681, email: [renan.rojasg,prodrig]@pucp.edu.pe

ABSTRACT

Automated selection of the regularization parameter for Total Variation restoration has shown to give very accurate reconstruction results. Most of the literature is devoted to the ℓ^2-TV case (images corrupted with Gaussian noise), whereas for the ℓ^1-TV case (images corrupted with salt-and-pepper noise) there are only a couple of published algorithms.

In this paper we present a computationally efficient algorithm for ℓ^1-TV denoising of grayscale and color images, which spatially adapts its regularization parameter. The proposed algorithm, which is based on the Iteratively Reweighted Norm algorithm, uses an adaptive median filter to initially estimate the outliers of the noisy (observed) image, and then proceeds to solve the ℓ^1-TV problem only for the noisy pixels while spatially adapts the regularization parameter based on local statistics. The experimental results show that the proposed method yields impressive results even when 90% of the image pixels are corrupted.

1. INTRODUCTION

Image denoising is a fundamental problem that consists in estimating the noise-free image from its corrupted (observed) version. Within the Total Variation (TV) framework, the salt-and-pepper noise model have been widely studied [1, 2, 3]. The ℓ^1-TV problem (as is commonly refered) has attracted considerable interest from the algorithmic point of view ([2, 3, 4, 5, 6, 7, 8] among others) due to the challenging nature of the cost functional it needs to minimize:

$$\min_{\mathbf{u}} T(\mathbf{u}) = \left\| \mathbf{u} - \mathbf{b} \right\|_1 + \lambda \left\| \sqrt{\sum_{n \in C} (D_x \mathbf{u}_n)^2 + (D_y \mathbf{u}_n)^2} \right\|_1, \quad (1)$$

where both the fidelity ($\|\mathbf{u} - \mathbf{b}\|_1$) and regularization ($\| \sqrt{\sum_{n \in C} (D_x \mathbf{u}_n)^2 + (D_y \mathbf{u}_n)^2} \|_1$) terms use the ℓ^1 norm and $\mathbf{u}_n$ represents each channel of $\mathbf{u}$. We note that if $C = \{1\}$, then $\mathbf{b}$ represents a grayscale noisy image; whereas if $C = \{1, 2, 3\}$, then $\mathbf{b}$ represents a color noisy image and $\mathbf{u}_n$ each channel of $\mathbf{u}$ and $\lambda \in \mathbb{R}$, $\lambda > 0$ represents the (global) regularization parameter.

The original ℓ^1-TV problem (1) features a single regularization parameter (λ), which influences the entire pixel set and has a direct impact on the quality of the reconstructed data. Ideally, for the salt-and-pepper noise model, noise-free pixels should preserve their values. However, the use of a global parameter forces the entire pixel set to be penalized, which results in an innacurate reconstruction. Typically, this parameter is manually selected in order to try to obtain the best possible reconstruction quality, based on a specific metric.

To the best of our knowledge, [9, 10] are the only published papers that tackle the above mentioned shortcomings for the ℓ^1-TV problem (for methods that adapt the regularization parameter for the ℓ^2-TV problem, we refer the reader to [11, 12, 13] and references therein). Whereas in [9], the original ℓ^1-TV problem is applied only on a set of corrupted-pixel candidates, which is estimated via an adaptive median filter. Here, the regularization parameter is manually selected. In [10] a scheme is proposed to spatially adapt the regularization parameter based only on local statistics and noise level estimation. Nevertheless, all pixels are still regularized.

In this paper we propose to combine two key ideas presented in [9, 10]: (i) find an estimate of the corrupted-pixel set, and (ii) automatically select and adapt the regularization based on local statistics. We stress that while in [9] a slightly modified ℓ^1-TV problem (as originally described in [2]) is actually solved, and in [10] the authors propose an unified Moreau-Yosida ([14, 15]) based primal-dual algorithm to solve (1), we propose to solve the modified ℓ^1-TV problem:

$$\min_{\mathbf{u}} T(\mathbf{u}) = \left\| \Lambda^{-1}(\mathbf{u} - \mathbf{b}) \right\|_1 + \left\| \sqrt{\sum_{n \in C} (D_x \mathbf{u}_n)^2 + (D_y \mathbf{u}_n)^2} \right\|_1, \quad (2)$$

by using the proposed algorithm, which is based on the Iteratively Reweighted Norm algorithm [7, 8]. In this equation, Λ is a diagonal matrix that represents the set of local regularization parameters. Note that if $\Lambda = \mathrm{diag}(\lambda)$, then (2) is equivalent to (1). The value of each element of Λ is automatically chosen via an iterative scheme based on noise-corrupted pixel candidates. Initial parameter values are defined based on a local noise level estimation. Then, local statistical information about the residual image is iteratively used to spatially adapt them. This approach requires no information about the noise-free image.

2. PRELIMINARY REMARKS

2.1 Technicalities

We represent 2-dimensional images by 1-dimensional vectors: $\mathbf{u}_n$ ($n \in C$) is a 1-dimensional (column) or 1D vector that represents a 2D grayscale image obtained via any ordering (although the most reasonable choices are row-major or column-major) of the image pixels. For $C = \{1, 2, 3\}$ we have that $\mathbf{u} = [(\mathbf{u}_1)^T (\mathbf{u}_2)^T (\mathbf{u}_3)^T]^T$ is a 1D (column) vector that represents a 2D color image.

The term $\frac{1}{q} \left\| \sqrt{\sum_{n \in C} (D_x \mathbf{u}_n)^2 + (D_y \mathbf{u}_n)^2} \right\|_q^q$ in (2) is the generalization of TV regularization to color images ($n \in$

$C = \{1,2,3\}$) with coupled channels (see [16, Section 9], also used in [17] among others), where we note that $\sqrt{\sum_{n\in C}(D_x\mathbf{u}_n)^2 + (D_y\mathbf{u}_n)^2}$ is the discretization of $|\nabla\mathbf{u}|$ for coupled channels (see [17, eq. (3)]), and D_x and D_y represent horizontal and vertical discrete derivative operators respectively.

2.2 Salt-and-pepper Noise Model

An observed vector-valued image with L channels $\mathbf{b}$ and elements $\mathbf{b}_n$ ($n \in C$) corrupted with salt-and-pepper noise is characterized by

$$b_n(k) = \begin{cases} \mathrm{v}_{min}, & \text{with probability } p_1 \\ \mathrm{v}_{max}, & \text{with probability } p_2 \\ u_n^*(k), & \text{with probability } 1-p_1-p_2 \end{cases} \quad (3)$$

where $u_n^*(k)$ describes a pixel in the noise-free image $\mathbf{u}^*$ and $p = p_1 + p_2$ represents the noise level.

2.3 Previous Related work

2.3.1 ℓ^1-TV methods based on local regularization parameters

In [9], pixel neighborhoods in the image of interest are analyzed to estimate the noise-corrupted pixel set $\mathcal{N}$. This regions are defined as:

$$\mathbf{s}_n(l,k) = b_n(k), \quad k \in \mathcal{K}_{w_n^l}(l), \quad (4)$$

where $\mathcal{K}_{w_n^l}(l)$ is the pixel set included in a $(2\cdot w_n^l + 1)\times(2\cdot w_n^l + 1)$ window centered at l, which is the pixel of interest. If w_n^l is not large enough to correctly analyze the pixel's condition, it is increased and the analysis is repeated. This procedure is part of an adaptive median filter algorithm (see [9, Algorithm 1]), which applies the slightly modified ℓ^1-TV problem described in [2] only on $\mathcal{N}$ by using a smooth approximation of the ℓ^1 norm, along with an artificial time marching scheme. The regularization parameter is manually selected. Although the quality of the reconstructed images is very good, the computational performance of the resulting algorithm is rather poor.

In [10] the authors propose an unified Moreau-Yosida [14, 15] based primal-dual algorithm to solve (1) for vector-valued images (the resulting algorithm is also capable of solving the ℓ^2-TV problem), by employing an estimate of the noise level p (see (3)) along with some initial guess to spatially adapt the regularization parameter based on a local noise estimator of the residual image. A window of fixed (arbitrary) size w (equal to eight pixels using the current notation) is used for such purpose. The reconstructed (color) images shows evident visual artifacts.

2.3.2 Iteratively Reweighted Norm (IRN) Algorithm

The IRN algorithm [7, 8] is a computationally efficient and flexible method that can handle the norms $p > 0$ and $q \le 2$ in the regularization and fidelity terms respectively, including the ℓ^2-TV and ℓ^1-TV for grayscale and color images as special cases by representing the ℓ^p and ℓ^q norms by their equivalent weighted ℓ^2 norms. This iterative problem is expressed as:

$$\min_{\mathbf{u}} T^{(k)}(\mathbf{u}) = \frac{1}{2}\left\| W_F^{(k)^{1/2}}(\mathbf{u}-\mathbf{b})\right\|_2^2 + \frac{\lambda}{2}\left\| W_R^{(k)^{1/2}} D\mathbf{u}\right\|_2^2, \quad (5)$$

and it converges to the solution of (1), where $W_F^{(k)} = \mathrm{diag}\left(\tau_{F,\epsilon_F}(\mathbf{u}^{(k)}-\mathbf{b})\right)$ and

$$D = I_L \otimes [Dx^T\, Dy^T]^T \quad W_R^{(k)} = I_{2L}\otimes\Omega^{(k)}, \quad (6)$$

$$\Omega^{(k)} = \mathrm{diag}\left(\tau_{R,\epsilon_R}\left(\sum_{n\in C}(D_x\mathbf{u}_n^{(k)})^2 + (D_y\mathbf{u}_n^{(k)})^2\right)\right), \quad (7)$$

where I_L is an $L\times L$ identity matrix, $\otimes$ is the Kronecker product, $C = \{1\}$, $L = 1$ or $C = \{1,2,3\}$, $L = 3$. Following a common strategy in IRLS type algorithms, the functions $\tau_{F,\epsilon_F}(x)$ and $\tau_{R,\epsilon_R}(x)$ are defined to avoid numerical problems (see [7, eqs. (5) and (12)]) when $\mathbf{u}^{(k)} - \mathbf{b}$ or $\sum_{n\in C}(D_x\mathbf{u}_n^{(k)})^2 + (D_y\mathbf{u}_n^{(k)})^2$ has zero-valued components.

3. SPATIALLY ADAPTIVE IRN ALGORITHM

In this section, we describe how to use the IRN algorithm to solve (2). Then, a summary of the noise-corrupted pixel set estimation and parameter update strategy is presented. Finally, the spatially adaptive IRN algorithm is listed.

3.1 Derivation

It is straighforward to check that if Λ is fixed we can use the IRN algorithm to solve (2). The equivalent weighted ℓ^2 version of the modified ℓ^1-TV problem can be written as:

$$\min_{\mathbf{u}} T^{(k)}(\mathbf{u}) = \frac{1}{2}\left\| W_F^{(k)^{1/2}}\Lambda^{(k)^{-1/2}}(\mathbf{u}-\mathbf{b})\right\|_2^2 + \frac{1}{2}\left\| W_R^{(k)^{1/2}} D\mathbf{u}\right\|_2^2, \quad (8)$$

where $\Lambda^{(k)} > 0$ is a diagonal matrix defined in some fashion. Since (8) is quadratic and its Hessian $\nabla^2 T^{(k)}(\mathbf{u}) = \left(W_F^{(k)}\Lambda^{(k)^{-1}} + D^T W_R^{(k)} D\right)$ is greater than zero, then the minimum of (2) can be reached by iteratively solving

$$\left(W_F^{(k)}\Lambda^{(k)^{-1}} + D^T W_R^{(k)} D\right)\mathbf{u} = W_F^{(k)}\Lambda^{(k)^{-1}}\mathbf{b}. \quad (9)$$

Finally, we mention that although (9) is mathematically correct, from a numerical point of view it is better to solve

$$\left(I + \Lambda^{(k)} W_F^{(k)^{-1}}\left(D^T W_R^{(k)} D\right)\right)\mathbf{u} = \mathbf{b}. \quad (10)$$

since it was found to result in a large reduction in the required number of CG iterations [7]. In Algorithm 1 we list our resulting method.

3.2 Corrupted Pixel Candidate Selection

The salt-and-pepper noise detector based on the adaptive median filter applied in [9, Algorithm 1] is succinctly described. The set of noise-corrupted pixels of the observed image $\mathbf{b}$ with L channels is defined by:

$$\mathcal{N} : \{n \in C, l \in \Omega : \hat{b}_n^{w_n^l}(l) \neq b_n(l) \wedge b_n(l) \in \{\mathrm{v}_{min}, \mathrm{v}_{max}\}\}, \quad (11)$$

where $\hat{b}_n^{w_n^l}(l)$ is the output of the Ranked Over Based Adaptive (RAMF) Filter [18]. This filter analyzes a $(2\cdot w_n^l+1)\times(2\cdot w_n^l+1)$ neighborhood centered at l in order to define whether this pixel is noise-corrupted or not. the neighborhood size is increased if the median of the neighborhood is equal to its minimum or maximun value, and the procedure is repeated until it reaches a maximum size w_{max}. Then, l is defined as a noise-corrupted pixel if it is equal to the maximum or minimum value in the neighborhood, in which case is replaced by the neighborhood's median.

In [9], manually selected values for w_{max} are applied depending on the noise level. Heuristically, we have determined that $w_{max}=9$ gives a good compromise between speed and reconstruction quality. w_n^l initial size is 1 for all l.

The proposed algorithm defines the set W, which is zero if the element l is noise-free and w_n^l if it is noisy. This gives information about the local noise level for each noise-corrupted pixel. Note that the global noise level p (see (3)) can be estimated as $\tilde{p}=\frac{1}{N}\sum \mathrm{I}_{[W\neq 0]}$, where N is the number of pixels and I is the indicator function.

3.3 Parameter Update

In [10] an estimation of local statistics for a fixed, manually selected neighborhood size is applied in order to give an educated guess about the noise level of the residual ($\mathbf{r}=\mathbf{u}-\mathbf{b}$) along with a sophisticated rule [10, eq. (3.2)] to spatially update the regularization parameters. For the spatially adaptive IRN algorithm, we also make use of local statistics of the residual, but based on particular neighborhood sizes (see section 3.2).

We define the local noise estimator as:

$$\hat{p}_n(l)=\frac{1}{M}\sum_{k\in\mathcal{K}_{w_n^l}(l)}|r_n(l)| \tag{12}$$

where $M=(2\cdot w_n^l+1)^2$ and $\mathcal{K}_{w_n^l}(l)$ is defined as in (4). The spatially dependant regularization parameter Λ is initialized as $\Lambda^{(0)}=\mathrm{diag}(\boldsymbol{\lambda}^{(0)})$, with $\lambda^{(0)}(l)=\mathrm{diag}(\mathrm{I}_{[w_n^l(l)>0]})+10^{-6}\,\mathrm{diag}(\mathrm{I}_{[w_n^l(l)==0]})$. After solving (2) via (10), we compute $\hat{p}_n(l)$ in order to obtain the regularization parameter updates $\lambda_n^{(m)}(l)$ in a spatially dependant fashion:

$$\lambda_n^{(m)}(l)=\begin{cases}\rho^{-1}\cdot\lambda_n^{(m-1)}(l) & \text{if } \hat{p}_n(l)<\tilde{p}\cdot\sigma\\ \rho\cdot\lambda_n^{(m-1)}(l) & \text{if } \hat{p}_n(l)>\tilde{p}\cdot\sigma\end{cases}, \tag{13}$$

where ρ,σ are constant values and $\tilde{p}$ is the estimated global noise level. Heuristically, we have found that $\rho\in[0.65,0.95],\sigma\in[0.25,0.5]$ gives good reconstruction results with just a few iterations (outer-loops in algorithm 1).

4. EXPERIMENTAL RESULTS

We compare the spatially adaptive IRN algorithm with the results reported for Algorithm III proposed in [9], which here is refered as *CHN*, and with the (standard) IRN algorithm [7, 8]. The test images consists of Lena (grayscale and color), Bridge (grayscale), and Goldhill (color). They are shown in Fig. 1 (except grayscale Lena). The test images were corrupted with a variable noise level: from 10% to 90%, with steps of 20%, which matches the experimental

Algorithm 1 Spatially Adaptive IRN algorithm for ℓ^1-TV

Initialize

Estimate set W from $\mathbf{b}$

$\Lambda^{(0)}=\mathrm{diag}(\mathrm{I}_{[w_n^l(l)>0]})+10^{-6}\,\mathrm{diag}(\mathrm{I}_{[w_n^l(l)==0]})$

$\mathbf{u}^{(0,0)}=\left(I+\Lambda^{(0)}D^TD\right)^{-1}\mathbf{b}$

for $m=0,1,..,\mathbf{M}$

  for $k=1,2,..,\mathrm{K}$

    $W_F^{(k)}=\mathrm{diag}\left(\tau_{F,\epsilon_F}(\mathbf{u}^{(m,k-1)}-\mathbf{b})\right)$

    $\Omega_R^{(k)}=\mathrm{diag}\left(\tau_{R,\epsilon_R}\left((D_x\mathbf{u}^{(m,k-1)})^2+(D_y\mathbf{u}^{(m,k-1)})^2\right)\right)$

    $W_R^{(k)}=\begin{pmatrix}\Omega_R^{(k)} & 0\\ 0 & \Omega_R^{(k)}\end{pmatrix}$

    $\mathbf{u}^{(m,k)}=\left(I+\Lambda^{(m)}{W_F^{(k)}}^{-1}D^TW_R^{(k)}D\right)\mathbf{b}$

  end

  $\mathbf{r}=\mathbf{u}^{(m,\mathrm{K})}-\mathbf{b}$

  estimate $\hat{\mathbf{p}}$ (via (12))

  compute $\Lambda^{(m+1)}$ (via (13))

end

setup in [9]. The quality metrics employed for evaluating the spatially adaptive IRN algorithm are: SNR= $10\log_{10}\frac{\mathrm{N}\sigma^2\{\mathbf{u}^*\}}{\|\mathbf{u}-\mathbf{u}^*\|_2^2}$, PSNR= $10\log_{10}\frac{\mathrm{N}(\max\{\mathbf{u}\})^2}{\|\mathbf{u}-\mathbf{u}^*\|_2^2}$, and SSIM [19], where N represents the number of elements contained in the image entire channel set. All simulations have been carried out using Matlab-only code on a 3GHz Intel core i7 CPU (L2: 1024K, RAM: 4G). Results corresponding to the IRN and the spatially adaptive IRN algorithm presented here may be reproduced using the the NUMIPAD (v. 0.30) distribution [20], an implementation of IRN and related algorithms.

(a) (b) (c)

Figure 1: Test image set: (a) color Lena (512x512 px.). (b) Bridge (720x576 px.). (c) Goldhill (512x512 px.).

For all experiments we use $w_{\max}=9$ (see section 3.2), and $\rho=0.65$ and $\sigma=0.5$ (see (13)) Also, we use five outer-loops with eight inner-loops ($M=5$ and $K=8$ in Algorithm 1), which seems to be a good compromise between the computational cost and the reconstruction quality.

As expected, both the CHN and the spatially adaptive IRN algorithm outperform the (standard) IRN algorithm. We also note that the CHN and the proposed algorithm have very similar performance for the grayscale case since both share the corrupted-noise detection method. Table 1 summarizes the ten-trial average of the reconstruction metrics for the IRN, the spatially adaptive IRN algorithm, and for CHN algorithm (where data is available). Figs. 2-4 show

the noisy test images, and their respective reconstruction images, based on the spatially adaptive IRN algorithm, for a noise level of 70% and 90%.

The execution time for the proposed algorithm is split into two specific tasks: Corrupted-pixel set detection and Iterative Minimization based on the IRN algorithm. Table 2 shows that the iterative procedure has a predominant weight in the computational time, although the noise detection step increases with the noise level, which is expected. Moreover, the computational performance of the spatially adaptive IRN outperforms that of the CHN algorithm ([9, Table II]) by a factor of 100 to 1 for images with 70% and 90% of noise corruption. Considering a correction factor for the CPUs available six years ago ([9] was published in 2005), this is still a significant computational improvement.

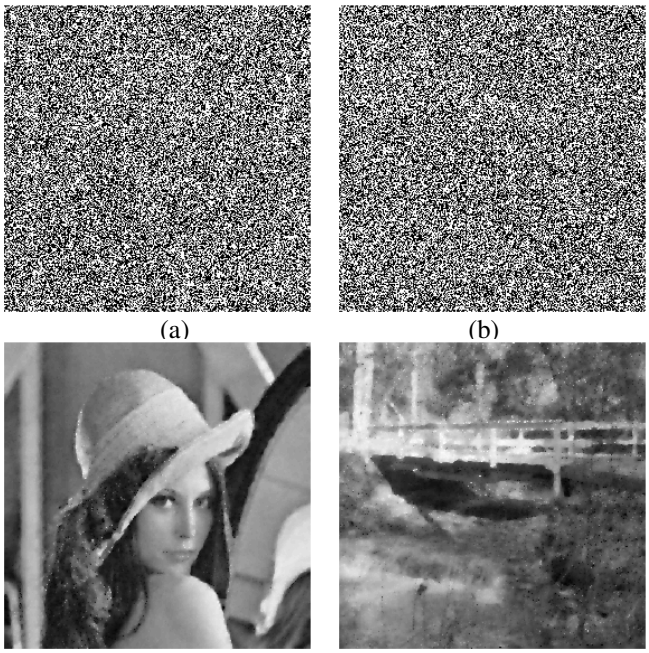

Figure 2: Image denoising for grayscale images: (a) 90% noise corrupted Lena. (b) 90% noise corrupted Bridge. (c) Reconstructed Lena. (d) Reconstructed Bridge.

5. CONCLUSIONS

The spatially adaptive IRN algorithm proposed in this paper has shown to accomplish high quality reconstructions for the salt and pepper noise scenario; it does not need any apriori information about the noise statistics nor any manually selected regularization parameters. The computational results show an outstanding structural preservation for noise levels up to 90%. Moreover, this method is performed in a simple but computationally efficient fashion, with a huge computational improvement (up to two orders of magnitude) over the previously developed methodology. The utilization of local parameters introduces a substantial effect in the reconstruction quality, while the adaptability feature allows to reach optimal quality values in an iterative but fast and accurate fashion, making this method comparable with the state of the art algorithms.

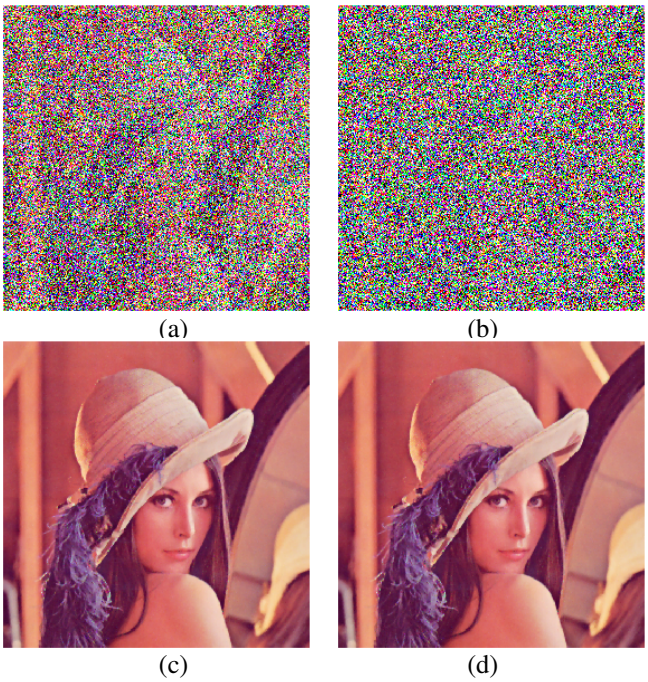

Figure 3: Image denoising for color Lena: (a) 70% noise corrupted. (b) 90% noise corrupted. (c) Reconstructed image for 70% noise level. (d) Reconstructed image for 90% noise. level

REFERENCES

[1] M. Nikolova, "Minimizers of cost-functions involving nonsmooth data-fidelity terms. application to the processing of outliers," *SIAM J. Numerical Analysis*, vol. 40, no. 3, pp. 965–994, 2002.

[2] M. Nikolova, "A variational approach to remove outliers and impulse noise," *J. of Math. Imag. and Vision*, vol. 20, pp. 99–120, 2004.

[3] T. Chan and S. Esedoglu, "Aspects of total variation regularized L^1 function approximation," *SIAM J. Appl Math*, vol. 65, no. 5, pp. 1817–1837, 2005.

[4] A. Chambolle, "Total variation minimization and a class of binary MRF models," *5th Int. Workshop on Energy Minimization Methods in Computer Vision and Pattern Recognition*, vol. 3757, pp. 136–152, 2005.

[5] J. Darbon and M. Sigelle, "Image restoration with discrete constrained total variation part I: Fast and exact optimization," *J. of Math. Imag. and Vision*, vol. 26, no. 3, pp. 261–276, 2006.

[6] L. Bar, A. Brook, N. Sochen, and N. Kiryati, "Deblurring of color images corrupted by impulsive noise," *IEEE TIP*, vol. 16, pp. 1101–1111, 2007.

[7] P. Rodríguez and B. Wohlberg, "Efficient minimization method for a generalized total variation functional," *IEEE TIP*, vol. 18, no. 2, pp. 322–332, 2009.

[8] P. Rodríguez and B. Wohlberg, "A generalized vector-valued total variation algorithm," in *Proceedings of ICIP*, Nov. 2009, pp. 1309–1312.

[9] R. Chan, C. Ho, and M. Nikolova, "Salt-and-pepper noise removal by median-type noise detectors and

Table 1: Computation of the reconstructed image quality reached by the spatially adaptive IRN algorithm, the standard IRN algorithm, and the CHN algorithm.(1) Information taken from [9, Fig. 2 - Fig. 5]. Results shown in dB.

Image	Noise	SNR (dB.)		PSNR (dB.)			SSIM [19]	
		IRN	SA-IRN	IRN	SA-IRN	CHN(1)	IRN	SA-IRN
Lena (gray)	0.5	12.8734	19.9870	26.4388	34.1221	≈34	0.8074	0.9419
	0.7	10.1669	16.4732	23.5971	30.6190	29.3	0.7283	0.8934
	0.9	2.3549	11.5379	14.3488	25.4222	25.4	0.5249	0.7760
Bridge (gray)	0.5	8.5561	13.8882	21.7991	27.1569	≈27	0.4941	0.8611
	0.7	7.0238	11.1691	20.0541	24.4027	25	0.3908	0.7396
	0.9	2.0901	7.6764	13.0018	20.9045	21.5	0.2371	0.4920
Lena (color)	0.5	16.2371	21.8106	28.9538	34.5205	–	–	–
	0.7	12.6595	18.7444	25.3708	31.4553	–	–	–
	0.9	2.8881	14.1123	15.1128	26.7976	–	–	–
Goldhill (color)	0.5	15.2090	20.4090	27.6639	32.9757	–	–	–
	0.7	12.0941	17.3832	24.8784	30.0075	–	–	–
	0.9	2.3510	13.2910	14.7308	25.7874	–	–	–

Table 2: Processing time for the spatially adaptive IRN algorithm. Results shown in seconds.

Noise level	Lena (gray)		Bridge (gray)		Lena (color)		Goldhill (color)	
	N. detector	Iter. ℓ-1 TV	N. detector	Iter. ℓ-1 TV	N. detector	Iter. ℓ-1 TV	N. detector	Iter. ℓ-1 TV
0.1	0.65	23.35	0.89	32.25	1.99	80.41	3.17	131.40
0.3	1.91	28.30	2.18	35.04	5.87	95.95	9.36	164.29
0.5	3.54	32.93	3.81	35.69	10.95	119.69	17.46	198.26
0.7	6.23	41.61	6.53	42.79	18.92	144.26	29.86	241.40
0.9	14.40	57.74	14.72	56.5	43.88	211.11	69.26	339.96

detail-preserving regularization," *IEEE TIP*, vol. 14, no. 10, pp. 1479–1485, 2005.

[10] Y. Dong, M. Hintermüller, and M. Rincon-Camacho, "Automated regularization parameter selection in multi-scale total variation models for image restoration," *Journal of Mathematical Imaging and Vision*, vol. 40, pp. 82–104, 2011.

[11] D. Strong and T. Chan, "Spatially and scale adaptive total variation based regularization and anisotropic diffusion in image processing," Tech. Rep., Division in Image Processing, UCLA Math Department, 1996.

[12] S. Ramani, T. Blu, and M. Unser, "Monte-carlo sure: A black-box optimization of regularization parameters for general denoising algorithms," *IEEE TIP*, vol. 17, no. 9, pp. 1540–1554, 2008.

[13] Y. Lin, B. Wohlberg, and H. Guo, "Upre method for total variation parameter selection," *IEEE Signal Processing*, vol. 90, no. 8, pp. 2546–2551, Aug. 2010.

[14] J. Moreau, "Proximité et dualité dans un espace hilbertien," *Bulletin de la Société Mathématique de France*, pp. 273–299, 1965.

[15] K Yosida, *Functional Analysis*, Springer Verlag, 4th ed. edition, 1974.

[16] A. Bonnet, "On the regularity of edges in image segmentation," *Annales de l'institut Henri Poincaré (C) Analyse non linéaire*, vol. 13, no. 4, pp. 485–528, 1996.

[17] X. Bresson and T. Chan, "Fast dual minimization of the vectorial total variation norm and applications to color image processing," *J. of Inverse Problems and Imaging*, vol. 2, no. 4, pp. 455–484, 2008.

[18] H. Hwang and R. Haddad, "Adaptive median filters: New algorithms and results," *IEEE Transactions on Image Processing*, pp. 499–502, 1995.

[19] Z. Wang, A. Bovik, H. Sheikh, and E. Simoncelli, "Perceptual image quality assessment: From error visibility to structural similarity," *IEEE TIP*, vol. 13, no. 4, pp. 600–612, April 2004.

[20] P. Rodríguez and B. Wohlberg, "Numerical methods for inverse problems and adaptive decomposition (NUMIPAD)," `http://numipad.sourceforge.net/`.

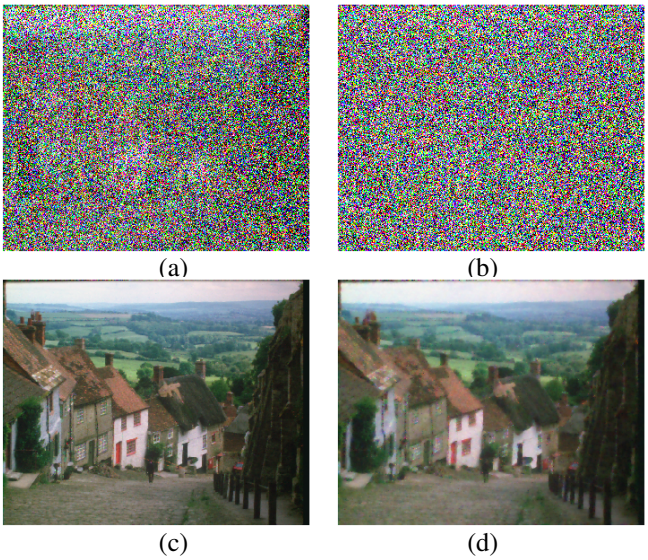

Figure 4: Image denoising for Goldhill: (a) 70% noise corrupted. (b) 90% noise corrupted. (c) Reconstructed image for 70% noise level. (d) Reconstructed image for 90% noise level.